

Laboratory Spectroscopic Studies of K-H₃O-Na Jarosite Solid Solutions Relevant to Mars. Changqing Liu¹ and Zongcheng Ling^{1*}, ¹Institute of Space Sciences, Shandong Provincial Key Laboratory of Optical Astronomy and Solar-Terrestrial Environment, Shandong University, Weihai 264209, China. (liuchangqing_td@126.com, zcling@sdu.edu.cn)

Introduction: Occurrence of jarosite and their global distributions on Mars are confirmed by *in-situ* [1-4] (e.g., Opportunity and Curiosity) and orbital remote sensing detections[5-10], indicating the odds of ephemeral, acidic fluids in Martian history. H₃O-bearing jarosite (H₃OFe₃(SO₄)₂(OH)₆) was detected using visible and near-infrared (VNIR) spectra from CRISM in Melas Chasma, which was the first orbital detection of jarosite, implying a regionally extensive aqueous alteration and low-temperature acidic conditions in the late Hesperian or possibly the Amazonian [6,7]. K-bearing jarosite (KFe₃(SO₄)₂(OH)₆) was found in Mawrth Vallis region, implying a limited supply of water in Martian history [8]. Na-bearing jarosite was identified in Noctis Labyrinthus, which might result from the partial acidic dissolution of Fe-smectite [9]. However, detailed chemical compositions of jarosite solid solutions are still ambiguous for Mars studies, which may lead to incomplete phase identifications and inaccuracy of evaluating local hydrothermal conditions.

In this study, we have synthesized 25 jarosite samples with different K-Na-H₃O contents, and derived three equations to assess the percentages of K, Na and H₃O contents in jarosite samples by VNIR, which would provide a valuable database for current orbital remote sensing investigations on Mars (e.g. CRISM).

Sample Preparations: We synthesized 22 jarosite solid solutions (JSS) and 3 jarosite endmembers (JED) under hydrothermal conditions in autoclaves at an incubator chamber at 140 °C. Samples were ground after the initial synthesis and reheated in the reactant solution until the sample was homogeneous based on multipoint analysis of Raman spectra. The exact chemical compositions were obtained by SEM-EDS (FEI Nova NanoSEM 450), indicated in Fig. 1.

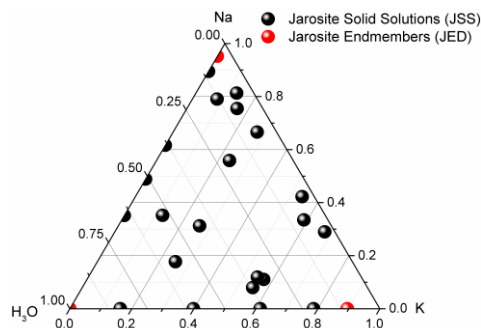


Fig. 1. Compositions of synthesized jarosite samples.

VNIR spectroscopy measurement: VNIR spectra were collected with FieldSpec® 4 Hi-Res VNIR spectrometer (Analytical Spectral Devices., Inc) from 350 to 2500 nm with spectral resolutions of 3 nm at visible region (350 to 1000 nm) and 8 nm at near-infrared region (1000 to 2500 nm) respectively. Before measurements, the spectrometer was calibrated by a Spectralon® panel with the highest diffuse reflectance over the ultraviolet, VNIR regions as a reflectance standard. A spectrum of each sample was obtained three times. Band centers were calculated by a Gaussian fit model.

Results and Discussion: VNIR spectra of all jarosite samples are shown in Fig. 2. Four distinct absorption features are obtained at ~890, ~1475, ~1850 and ~2270 nm, which are assigned as ⁶A_{1g} → ⁴T_{1g} transitions of Fe³⁺, 2ν(OH)⁻, ν(OH)⁻+2δ(OH)⁻, and ν(OH)⁻+2δ(OH)⁻, respectively.

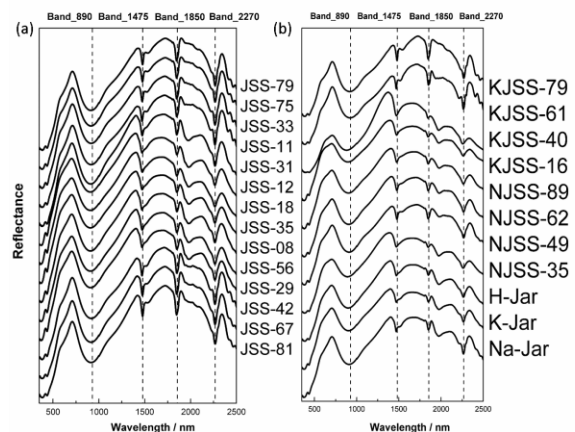


Fig. 2. VNIR spectra of synthesized jarosite samples. (JSS-11: K-Na-H₃O jarosite solid solution with 11% K; KJSS-61: K-H₃O jarosite solid solution with 61% K; NJSS-62: Na-H₃O jarosite solid solution with 62% Na)

Band centers of these features show systematic variations with K-number (K/(K+Na+H₃O)×100%), Na-number (Na/(K+Na+H₃O)×100%) and H₃O-number (H₃O/(K+Na+H₃O)×100%) in jarosite (Fig. 3). Band centers of absorption features at ~890, ~1850 and ~2270 nm shift to a shorter wavelength as increasing H₃O content. The feature at ~1475 nm exhibits a red shift as increasing Na and blue shift as an increasing portion of K. K-, Na- and H₃O-number in jarosite solid solutions and endmembers can be assessed as follows:

$$K\text{-number} = 0.883 \times \text{Band_890} - 5.086 \times \text{Band_147} + 9.768 \times \text{Band_1850} - 1.987 \times \text{Band_2270} - 6815.7 \quad (\text{Eq.1})$$

$$Na\text{-number} = -1.265 \times \text{Band_890} + 1.764 \times \text{Band_147} - 17.13 \times \text{Band_1850} + 10.101 \times \text{Band_2270} + 7327.89 \quad (\text{Eq.2})$$

$$H_3O\text{-number} = -1.269 \times \text{Band_890} + 0.17 \times \text{Band_147} + 0.914 \times \text{Band_1850} - 3.913 \times \text{Band_2270} + 8086.92 \quad (\text{Eq.3})$$

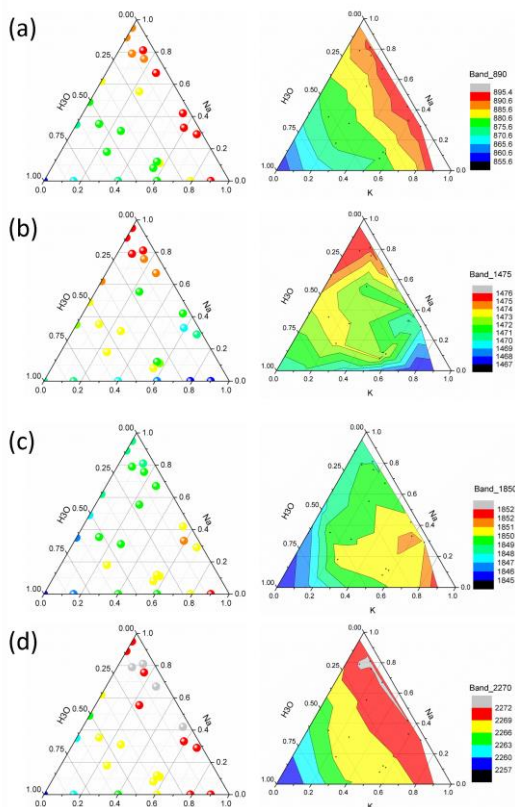


Fig. 3. Band center variations and contour with K, Na and H₃O compositions.

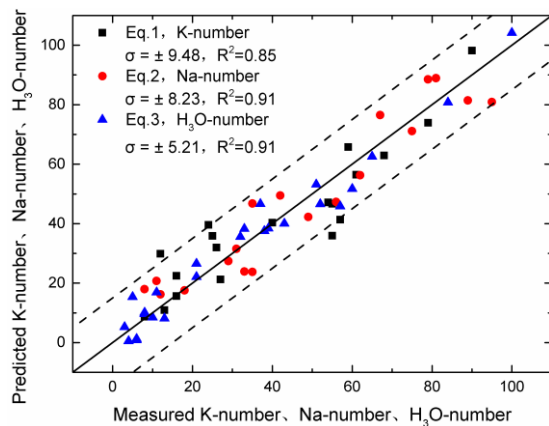


Fig. 4. Predicted K-number, Na-number, and H₃O-number confirmed by Eq.1, E1.2, and Eq.3 versus measured K-number, Na-number, and H₃O-number.

As shown in Fig. 4, the data points of measured and predicted K-number, Na-number, and H₃O-number in jarosite are almost along a 1:1 line, suggesting good predictions. The R-square values of the fitting are 0.85, 0.91 and 0.91 respectively, and the standard deviation between measured and predicted values are ± 9.48 , ± 8.23 and ± 5.21 (less than ± 10.0). These equations can be used as a tool for evaluating jarosite compositions on Mars using visible and near-infrared spectroscopy.

Future Work: We will extend researches on the spectral-compositional-structural trends utilizing more method, such as Raman spectra. We will predict jarosite compositions using remote sensing spectra (e.g., CRISM) in combination with a geochemical modeling method to better understand past water-rock interactions on Mars.

Acknowledgements: This research was supported by the National Natural Science Foundation of China (41473065), Natural Science Foundation of Shandong Province (JQ201511), Qilu (Tang) Young Scholars Program of Shandong University, Weihai (2015WHWLJH14).

References: [1] Christensen P. R. et al. (2004) *Science*, 306, 5702. [2] Klingelhofer G. et al. (2004) *Science*, 306, 1740. [3] Squyres S. W. et al. (2004) *Science*, 306, 1709. [4] Johnson J. R. et al. (2015) *Icarus* 249, 74. [5] Michalski J. R. et al. (2013) *Icarus*, 226, 816. [6] Milliken R. E. et al. (2008) *Geology*, 36, 847. [7] Metz J. M. et al. (2009) *Journal of Geophysical Research: Planets*, 114. [8] Farrand W. H. et al. (2009) *Icarus*, 204, 478. [9] Thollot P. et al. (2012) *Journal of Geophysical Research: Planets*, 117. [10] Stack K. M. et al. (2015) *Icarus*, 250, 332.